HHS Public Access

Author manuscript

Science. Author manuscript; available in PMC 2019 November 10.

Published in final edited form as:

Science. 2019 May 10; 364(6440): 588–592. doi:10.1126/science.aav4632.

Vision using multiple distinct rod opsins in deep-sea fishes

Zuzana Musilova[1,2,*,†], **Fabio Cortesi**[1,3,*,†], **Michael Matschiner**[1,4,5], **Wayne I. L. Davies**[6,7,8,9], **Jagdish Suresh Patel**[10,11], **Sara M. Stieb**[1,3,12], **Fanny de Busserolles**[3,13], **Martin Malmstrøm**[1,4], **Ole K. Tørresen**[4], **Celeste J. Brown**[11], **Jessica K. Mountford**[6,7,8], **Reinhold Hanel**[14], **Deborah L. Stenkamp**[11], **Kjetill S. Jakobsen**[4], **Karen L. Carleton**[15], **Sissel Jentoft**[4], **Justin Marshall**[3], and **Walter Salzburger**[1,4,†]

[1]Zoological Institute, Department of Environmental Sciences, University of Basel, Basel, Switzerland. [2]Department of Zoology, Charles University, Prague, Czech Republic. [3]Queensland Brain Institute, The University of Queensland, Brisbane, Australia. [4]Centre for Ecological and Evolutionary Synthesis (CEES), Department of Biosciences, University of Oslo, Oslo, Norway. [5]Department of Palaeontology and Museum, University of Zurich, Zurich, Switzerland. [6]UWA Oceans Institute, The University of Western Australia, Perth, Australia. [7]School of Biological Sciences, The University of Western Australia, Perth, Australia. [8]Lions Eye Institute, The University of Western Australia, Perth, Australia. [9]Oceans Graduate School, The University of Western Australia, Perth, Australia. [10]Center for Modeling Complex Interactions, University of Idaho, Moscow, USA [11]Department of Biological Sciences, University of Idaho, Moscow, USA. [12]Eawag, Swiss Federal Institute for Aquatic Science and Technology, Centre of Ecology, Evolution & Biogeochemistry, Department of Fish Ecology & Evolution, Kastanienbaum, Switzerland. [13]Red Sea Research Center (RSRC), Biological and Environmental Sciences & Engineering Division (BESE), King Abdullah University of Science and Technology (KAUST), Thuwal, Saudi Arabia. [14]Thünen Institute of Fisheries Ecology, Bremerhaven, Germany. [15]Department of Biology, University of Maryland, College Park, USA.

Abstract

Vertebrate vision is accomplished through light-sensitive photopigments consisting of an opsin protein bound to a chromophore. In dim-light, vertebrates generally rely upon a single rod opsin (RH1) for obtaining visual information. By inspecting 101 fish genomes, we found that three

[†]Corresponding authors. zuzana.musilova@natur.cuni.cz (Z.M.); fabio.cortesi@uqconnect.edu.au (F.C.); walter.salzburger@unibas.ch (W.S.).

[*]These authors contributed equally to this work.

Author Contributions: Z.M., F.C., J.M., and W.S. conceived the study; Mi.M., Ma.M., R.H., K.S.J., S.J. and W.S. planned and led the genome sequencing and provided samples; Z.M., F.C., F.d.B., J.M., and W.S. carried out transcriptome sequencing. Z.M. and F.C. carried out the opsin gene analyses. F.C. and S.M.S. performed the PGLS analyses. Mi.M., Ma.M., O.K.T., and S.J., carried out the genome assemblies and annotations. Mi.M. carried out phylogenetic analyses. K.L.C. performed the regulatory region analyses and visual modelling. W.I.L.D. and J.K.M. carried out the *in vitro* regeneration and spectral prediction analyses. J.S.P. performed the atomistic molecular simulations, and J.S.P., C.J.B., and D.L.S. generated, analyzed and interpreted the predictive model. All authors gave comments on the manuscript and approved the final version.

Competing interests: The authors declare no competing interests.

Data and materials availability. New draft genome sequences from this study are available at the European Nucleotide Archive (ENA; study accession number: PRJEB30779); transcriptomic data that support the findings of this study have been deposited on GenBank (BioProject ID PRJNA421052). Source files including custom scripts have been deposited in GitHub (https://github.com/mmatschiner/opsin_evolution), phylogenetic trees and sequence alignments are available at http://evoinformatics.eu/opsin_evolution.htm. All other data analyzed during this study are included as Supplementary Materials.

deep-sea teleost lineages have independently expanded their *RH1* gene repertoires. Amongst these, the silver spinyfin (*Diretmus argenteus*) stands out as having the highest number of visual opsins in vertebrates (2 cone, 38 rod opsins). Spinyfins express up to 14 *RH1*s (including the most blue-shifted rod photopigments known), which cover the range of the residual daylight as well as the bioluminescence spectrum present in the deep sea. Our findings present molecular and functional evidence for the recurrent evolution of multiple rod opsin-based vision in vertebrates.

Keywords

sensory systems; convergent evolution; gene duplication; teleosts; adaptations

Animals use vision for a variety of fundamental tasks including navigation, foraging, predator avoidance, and mate choice. At the molecular level, the process of vision is initiated through a light-induced conformational change in a photopigment (a visual opsin bound to a vitamin A-derived chromophore), which in turn activates the phototransduction cascade (1). Vertebrates possess up to five types of visual opsins, four opsins primarily expressed in cone photoreceptors in the retina and one opsin expressed in the rod photoreceptor (1). Cones generally operate in bright-light (photopic) conditions and are sensitive to a broad range of wavelengths: Photopigments containing the short-wavelength-sensitive opsins, SWS1 and SWS2, absorb in the ultraviolet [UV; peak spectral sensitivity (λ_{max})=355–450 nm] and violet/blue (λ_{max}=415–490 nm) regions of the spectrum, respectively; the middle-wavelength-sensitive RH2 is most sensitive to the central (green) waveband (λ_{max}=470–535 nm); and the long-wavelength-sensitive LWS is tuned towards the spectrum's red end (λ_{max}=490–570 nm) (1). Usually, vertebrates rely on 2–4 spectrally distinct cone photoreceptors for color opponency, i.e., the ability to distinguish different chromatic signals (2,3). Under dim-light (scotopic) conditions, most vertebrates are color-blind, relying upon their single rod photopigment (RH1) for obtaining achromatic visual information (1,3).

Here, we scrutinized the evolution of the visual opsin-gene repertoire of teleosts, with a particular focus on deep-sea fishes. These exhibit various adaptations to maximize their visual sensitivities in a scotopic environment where bioluminescence replaces surface illumination as the primary source of light (4,5), including increased eye or pupil sizes, reflective tapeta, or extremely modified tubular eye structures (6). Other modifications concern the retina itself with many deep-sea fishes having pure-rod retinae with elongated outer segments, and in some cases 'multibank retinae' in which rods are stacked in layers (7).

To examine molecular adaptations in the teleost visual system, we first reconstructed the visual opsin-gene loci in 100 teleosts (plus one non-teleost outgroup; Fig. 1; fig. S1; table S1) (8). We found that teleosts possess a median number of 7 visual opsin genes. This elevated number compared to other vertebrates (3) can primarily be attributed to an expansion of *SWS2* and *RH2*, which are sensitive to the most prevalent, blue-green part of the aquatic light spectrum. We found that 78 species had more than one *RH2* copy, and 53 species had at least one extra version of *SWS2* (see also ref. 9). Gene losses, on the other

hand, mainly affected the opsins sensitive to the edges of the visible light spectrum, *SWS1* (absent in 46 species) and *LWS* (absent in 34 species, of which 28 inhabit the deep sea).

A phylogenetic generalized least-squares (PGLS) analysis revealed that, while the total number of visual opsin genes was unaffected by phylogeny or depth at which a species occurs (Pagel's λ=0, $F_{1,74}$=0.32, p=0.57), deeper-dwelling species have significantly fewer *LWS* genes (Pagel's λ=1.0, $F_{1,74}$=38.47, p<0.0001) (table S2). In common with most vertebrates (3), the majority of teleosts possess a single *RH1* irrespective of phylogeny and depth (Pagel's λ=0, $F_{1,74}$=2.87, p=0.09). However, we identified 13 species with more than one *RH1* (see also ref. 10). Four deep-sea species from three distinct clades stand out by possessing 5 or more *RH1*s: The glacier lanternfish (*Benthosema glaciale*) with 5 *RH1*s, the tube-eye (*Stylephorus chordatus*) with 6 *RH1*s, and two species of the Diretmidae; the longwing spinyfin (*Diretmoides pauciradiatus*) with 18 and the silver spinyfin (*Diretmus argenteus*) with 38 *RH1*s (Fig. 1). In all cases, the *RH1* gene expansions occurred through single-gene rather than whole-genome duplications (fig. S2; table S3).

To determine which of the visual opsins are being used, we sequenced retinal transcriptomes of 36 species sampled across the teleost phylogeny. We found that the majority of species (n=24) express up to 4 cone opsins, despite having – in many cases – more opsin genes in their genomes (fig. S3). This is consistent with the use of 2–4 differently-tuned cone photoreceptors for color vision in the vast majority of vertebrates (11). The retinae of the remaining 12 species contained transcripts of 5–7 cone opsins (fig. S3), a pattern previously reported in some teleosts (3). We further found that deep-sea fishes with an extended *RH1* repertoire indeed express more than one *RH1*: the lanternfishes *B. glaciale* and *Ceratoscopelus warmingii* express three *RH1*s each, the tube-eye expresses five *RH1*s; and the silver spinyfin was found to express up to 7 and 14 *RH1*s as larvae and adults, respectively (Fig. 2A, table S4). A similarly high number of retinal opsin transcripts has previously only been reported from dragonflies (12) and stomatopod crustaceans (13), in the latter case generating up to 12 differently-tuned photoreceptor types.

In vertebrates, substitutions at 27 amino-acid positions have so far been implicated with the spectral tuning of RH1 photopigments via functional shifts in λ_{max} (1,3). Our ancestral-state reconstruction revealed that 25 out of these 27 known key spectral-tuning sites have been altered across teleosts (Fig. 3; fig. S4), and at 18 of these sites, the same amino-acid substitutions have occurred repeatedly in different lineages (table S5). The lineage-specific *RH1* expansion within Diretmidae alone gave rise to a set of genes differing in 24 key spectral-tuning sites (tables S5, S6). In addition, the *RH1* genes of Diretmidae show the, by far, highest non-synonymous to synonymous (dN/dS) substitution-rate ratios across all teleost *RH1*s (Fig. 3B; table S7), suggesting that the extensive occurrence of parallel substitutions was driven by adaptive sequence evolution.

Using *D. argenteus* as an example, we tested whether the deep-sea fish *RH1* expansions translate into differently-tuned photopigments. Predictions on the basis of regenerated proteins and molecular dynamics simulations (8) revealed that the *D. argenteus* RH1s cover a λ_{max}-range of 447–513 nm and 444–519 nm, respectively (Fig. 2B; figs. S5–S8; tables S8–S10). This peak-to-peak spectral range is much broader than that commonly found for

RH1 in other deep-sea fishes (λ_{max}=477–490 nm) and includes the most blue-shifted rod opsins known for vertebrates (14). However, this spectral range largely overlaps with both the waveband of bioluminescent light emitted by deep-sea organisms (λ=420–520 nm) (5) and the residual daylight at a depth of 500 m (λ=432–507 nm) (15). A function-through-time analysis inferred that the ancestral Diretmidae RH1 photopigment had a λ_{max} of ~472 nm, similar to the spectral peak of the rod photopigment in most extant deep-sea fishes (17). A subsequent gene-duplication event led to two versions of *RH1* that diverged rapidly in spectral sensitivity (λ_{max}~457 nm, 482 nm), which gave rise to all further *RH1*s (Fig. 2C,D). The emergence of the blue-shifted clade was likely caused by the loss of a key disulfide bridge between amino acid positions 111 and 188 (Fig. 3C, table S10, movies S1, S2), extending the list of known tuning sites.

The vastly expanded opsin-gene repertoire of Diretmidae is therefore intriguing, especially in the context of its retinal anatomy, the ventral (upward-directed) retina of *D. argenteus* containing extremely long rods as part of a multibank retina (16,17). Placing just the shortest-or the longest-tuned *D. argenteus* visual pigments within these rods results in very broad absorptance spectra that would not only overlay the spectra of the remaining RH1 pigments, but would already, on their own, maximize photon capture (fig. S9). This is also the case for the other examples of deep-sea fishes with multi-rod-opsin retinae (e.g., in Myctophidae and Stylephoridae), which also possess very long photoreceptors and, in some cases, multibank retinae (6,7). Notwithstanding the potential for any single photoreceptor to sample all available light, it is worthwhile exploring the possible functions of multiple spectral sensitivities in this environment. Five not necessarily exclusive scenarios could explain the *RH1* proliferation:

- **(i)** The sensitivity of individual photoreceptors may be (further) broadened by co-expression of multiple, differently-tuned RH1s across the ambient light spectrum; this could increase absolute sensitivity in scotopic conditions, as proposed for cone co-expression in nocturnal mammals (18).
- **(ii)** Sensitivity may be increased through summing the outputs of photoreceptors containing different spectral sensitivities, whether they contain one or more RH1s (6).
- **(iii)** Color discrimination may be possible if different spectral classes or combinations thereof are compared through an opponent process (17); although apparently representing ‘normal’ color vision, its mediation by rods containing RH1s and not by cones would be unique (19,20).
- **(iv)** Each spectral sensitivity or set of sensitivities may be hard-wired to a specific behavior, e.g., identification of a specific bioluminescent flash, a process termed wavelength-specific or unconventional color vision in other animals (21).
- **(v)** The range of spectral sensitivities act as a store of solutions that can be ‘pulled off the shelf’ at different developmental stages or placed in different retinal regions to optimize sensitivity and/or contrast of objects (21).

Supporting the existence of purely rod-based color vision in deep-sea fishes (*iii* and *iv*), members from the deep-sea lineages with expanded *RH1* repertoires have rod

photoreceptors with different spectral sensitivities and additional yellow spectral filters within the eye. These filters have been suggested to enhance color discrimination or at least contrast (22,23). Color vision in the deep sea may be advantageous to recognize spectrally diverse bioluminescent spectra (5). For example, it may help break bioluminescent camouflage against downwelling light for identifying conspecifics or prey (16).

While we are currently unable to behaviorally test any of these possibilities, theoretical visual models from the perspective of *D. argenteus* make some predictions (fig. S10; tables S11). Contrast detection of a black object (e.g., a fish silhouette) or a bioluminescent light source (e.g., a decapod prey) against the residual daylight requires just a single RH1 photopigment. However, for optimal detection of a black object, that pigment needs to be exactly matched to the background illumination, while a bioluminescent object demands a sensitivity slightly longer than the peak emission of the bioluminescence. Hence, several differently tuned photopigments would be beneficial for the detection of different bioluminescence sources (fig. S10B). Conversely, if two bioluminescent signals were to be distinguished from one another (i.e., a form of color vision), maximum discrimination would ideally be achieved using two photopigments matched to each bioluminescent emission. None of the models predict why having 14 functional sensitivities is useful; however, they do suggest that an exact sensitivity match to each specified task is an advantage. Possessing an adaptable system as suggested in (*v*) – during ontogeny or to optimize upward, downward, and side-facing vision – might require this sort of diversity of spectral classes.

In a fascinating parallel in the otherwise monochromatic cephalopods, the abraliopsid squids also express multiple visual-pigment types in multibank retinae and utilize differently-colored bioluminescent signals during seasonal mating (24). Whether bioluminescent signaling in the deep has driven the extreme diversity of spectral sensitivities in deep-sea fish or not, our findings help redefine the current paradigm of vertebrate vision in terms of the role of rod photoreceptors.

Supplementary Material

Refer to Web version on PubMed Central for supplementary material.

Acknowledgements

We thank Andrew Bentley, Michael Berenbrink, Wen-Sung Chung, Adrian Indermaur, Xabier Irigoien, Stein Kaartvedt, Lukáš Kalous, M. Danielle MacDonald, Jiří Peterka, Genevieve Phillips, Jan Yde Poulsen, Even Sannes Riiser, Anders Rostad, Olivia Roth, Ana Gro Salvanes, Helle Tessand Baalsrud and Lee Frey (HBOI/Blue Turtle Engineering) for their help in the field and/or for providing samples; the staff of the Lizard Island Research Station for logistical support; the captains and crews of the research vessels *Seward Johnson*, *Walther Herwig III*, *Sonne*, *G. O. Sars*, *Thuwal*, *Maria S. Merian,* and *Trygve Braarud* for the opportunity to participate and collect samples; the Norwegian Sequencing Centre (NSC), University of Oslo, and the McGill University and Génome Quebéc Innovation Centre for performing whole genome sequencing; Janette Edson (Queensland Brain Institute), Christian Beisel (D-BSSE, Basel), and Craig Michell (KAUST) and teams for help with transcriptome sequencing; the Center for scientific computing @ University of Basel (sciCORE) and the High Performance Computing Center at Idaho National Laboratory (supported by the Office of Nuclear Energy of the U.S. DOE and the Nuclear Science User Facilities under Contract No. DE-AC07–05ID14517) for computational resources; the Waitt Foundation for Discovery for hosting and support; Francesco Santini for discussions regarding fossil calibrations; and the anonymous referees for insightful comments and suggestions that improved the manuscript.

Funding: This work was funded by the Czech Science Foundation (16–09784Y), the Swiss National Science Foundation (SNF, 166550), and the Basler Stiftung für Experimentelle Zoologie to Z.M.; an SNF Postdoctoral

Fellowship (165364) and a UQ Development Fellowship to F.C.; a Future Fellowship (FT110100176) of the Australian Research Council (ARC) and a Discovery Project grant (DP140102117) to W.I.L.D.; the ARC to F.C. and J.M.; the Basler Stiftung für Biologische Forschung to Z.M. and S.M.S; the Research Council of Norway (RCN 222378) to K.S.J.; the Center for Modeling Complex Interactions sponsored by the NIGMS (P20 GM104420) and National Science Foundation EPSCoR Track-II (OIA1736253) to J.S.P.; KAUST to F.d.B.; the NIH (R01EY012146) to D.L.S.; the NIH (R01EY024639) to K.L.C.; The Deep Australia Project ARC LP0775179 to J.M.; and the European Research Council (ERC; CoG 'CICHLID~X') and the SNF (156405, 176039) to W.S.

REFERENCES AND NOTES

1. Yokoyama S, Annu. Rev. Genomics Hum. Genet. 9, 259–282 (2008). [PubMed: 18544031]
2. Lythgoe JN, The Ecology of Vision (Clarendon Press, 1979).
3. Hunt DM, Collin SP, in Evolution of Visual and Non-visual Pigments (eds. Hunt DM, Hankins MW, Collin SP, Marshall NJ) 163–217 (Springer, 2014).
4. Douglas RH, Partridge JC, Fish Biol J. 44, 68–85 (1997).
5. Widder EA, Science 328, 704–709 (2010). [PubMed: 20448176]
6. Warrant EJ, Locket NA, Biol. Rev. 79, 671–712 (2004). [PubMed: 15366767]
7. Wagner HJ, Frohlich E, Negishi K, Collin SP, Prog. Retin. Eye Res. 17, 637–685 (1998). [PubMed: 9777652]
8. Materials and methods are available as supplementary materials on Science Online.
9. Cortesi F, et al., Proc. Natl. Acad. Sci. USA 112, 1493–1498 (2015). [PubMed: 25548152]
10. Morrow JM, et al., J. Exp. Biol. 220, 294–303 (2017). [PubMed: 27811293]
11. Kelber A, Vorobyev M, Osorio D, Biol. Rev. Camb. Philos. Soc. 78, 81–118 (2003). [PubMed: 12620062]
12. Futahashi R, et al., Proc. Natl. Acad. Sci. USA 112, E1247–E1256 (2015) [PubMed: 25713365]
13. Porter ML, et al., Integr. Comp. Biol. 53, 39–49 (2013). [PubMed: 23727979]
14. Douglas RH, Partridge JC, Marshall NJ, Prog. Retin. Eye Res. 17, 597–636 (1998). [PubMed: 9777651]
15. Johnsen S, Ann. Rev. Mar. Sci. 6, 369–392 (2014).
16. Munk O, Videnskab. Meddr. Dansk. Naturh. Foren. 129, 73–80 (1966).
17. Denton EJ, Locket NA, J. Mar. Biol. Assoc. UK 69, 409–435 (1989).
18. Peichl L, Anat. Rec. A. Discov. Mol. Cell. Evol. Biol. 287, 1001–1012 (2005). [PubMed: 16200646]
19. Roth LS, Kelber A, Proc. R. Soc. B 271, S485–487 (2004).
20. C. A. Yovanovich, et al., Phil. Trans. R. Soc. B 372, 20160066 (2017).
21. Marshall J, Carleton KL, Cronin Curr T. Opin. Neurobiol. 34, 86–94 (2015).
22. De Busserolles F, et al., Brain Behav. Evol. 85, 77–93 (2015). [PubMed: 25766394]
23. Partridge JC, Archer SN, Vanoostrum J, Marine Biol J. Assoc. UK 72, 113–130 (1992).
24. Michinomae M, Masuda H, Seidou M, Kito Y, J. Exp. Biol. 193, 1–12 (1994). [PubMed: 9317205]

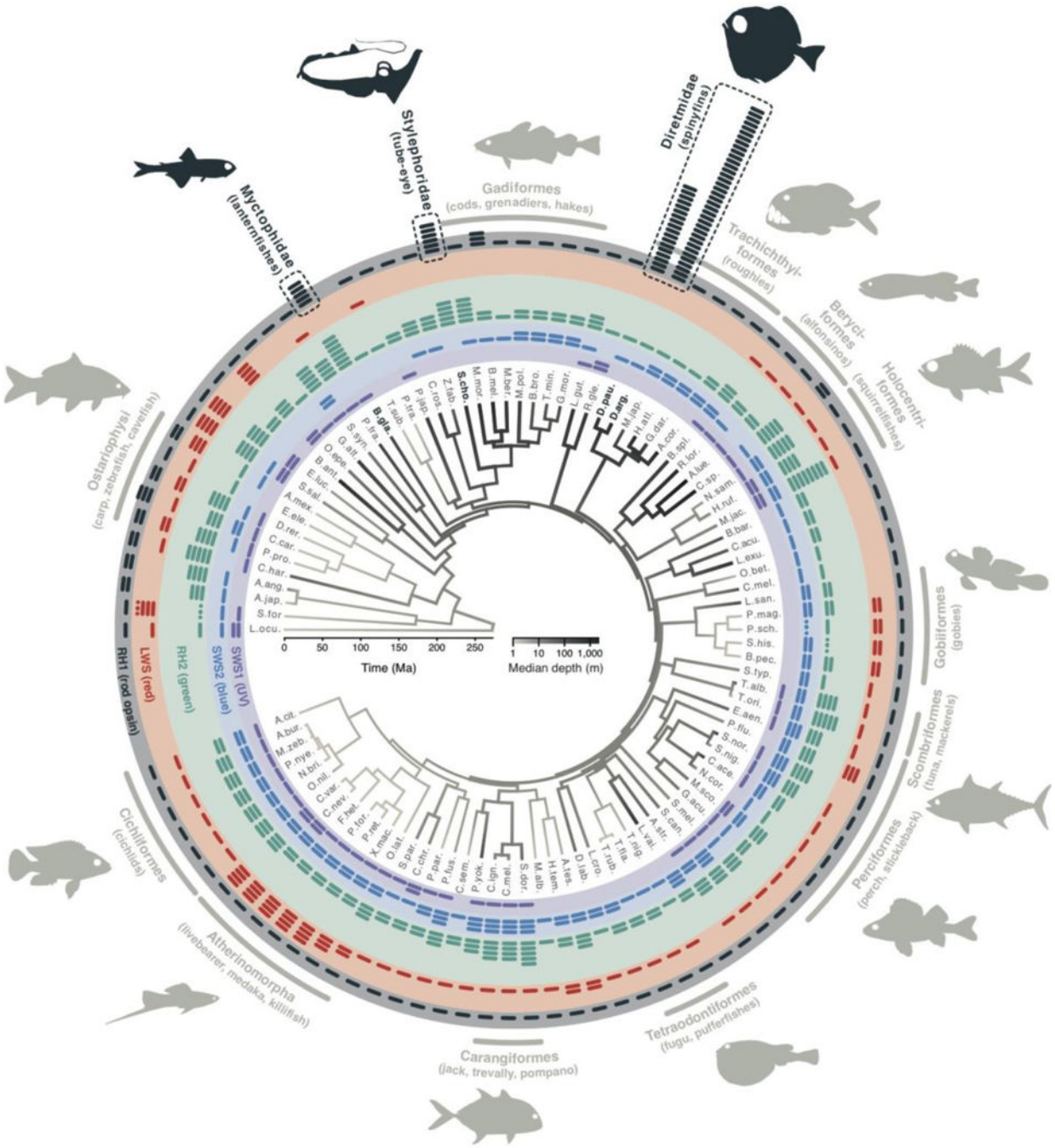

Fig. 1. Diversity of visual opsin genes in teleost fishes.

The time-calibrated phylogeny in the center is based on molecular information provided by 101 fish genomes and shaded according to the median depth of occurrence of each species (terminal branches) and reconstructed depths (internal branches). Colored bars in the outer circles indicate the number of cone opsin genes, while the number of rod opsins (*RH1*) is shown as black bars; dotted bars refer to incomplete or ambiguous data. Deep-sea lineages with multiple *RH1* copies are highlighted with dashed boxes. A detailed version of the phylogeny including full species names is provided in fig. S1.

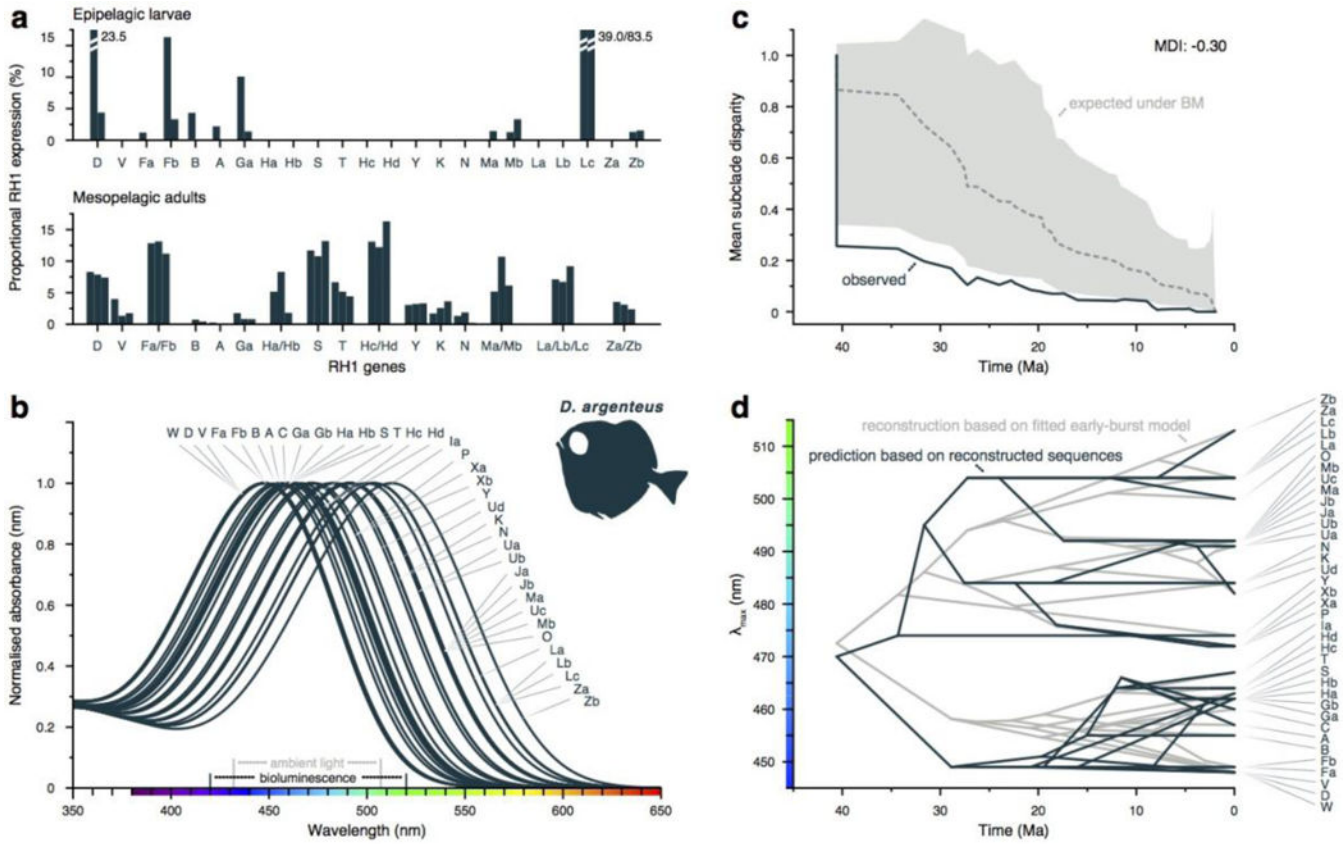

Fig. 2. Molecular function of rod photoreceptors in the silver spinyfin.

(A) Expression of *RH1* genes in the retina of epipelagic larvae (upper panel) and adults (lower panel). (**B**) Peak spectral sensitivities (λ_{max}) of 37 (out of 38) RH1s of *D. argenteus* based on *in vitro* protein regenerations (black) and subsequent key tuning-site predictions (gray). (**C**) Reconstruction of mean sub-clade disparity-through-time in λ_{max}-values for the RH1s of *D. argenteus* supporting an early burst (EB) scenario of diversification (AIC_{EB}=236.4) over time-homogenous diversification (Brownian Motion, BM; AIC_{BM}=244.9) or selection towards an optimal value of λ_{max} (Ornstein-Uhlenbeck model, OU, not shown; AIC_{OU}=246.9). (**D**) Functional divergence-through-time of λ_{max}-values according to predicted λ_{max}-values for reconstructed ancestral sequences (black) and ancestral λ_{max}-values reconstructed on the basis of an early-burst model (gray). MDI: morphological disparity index.

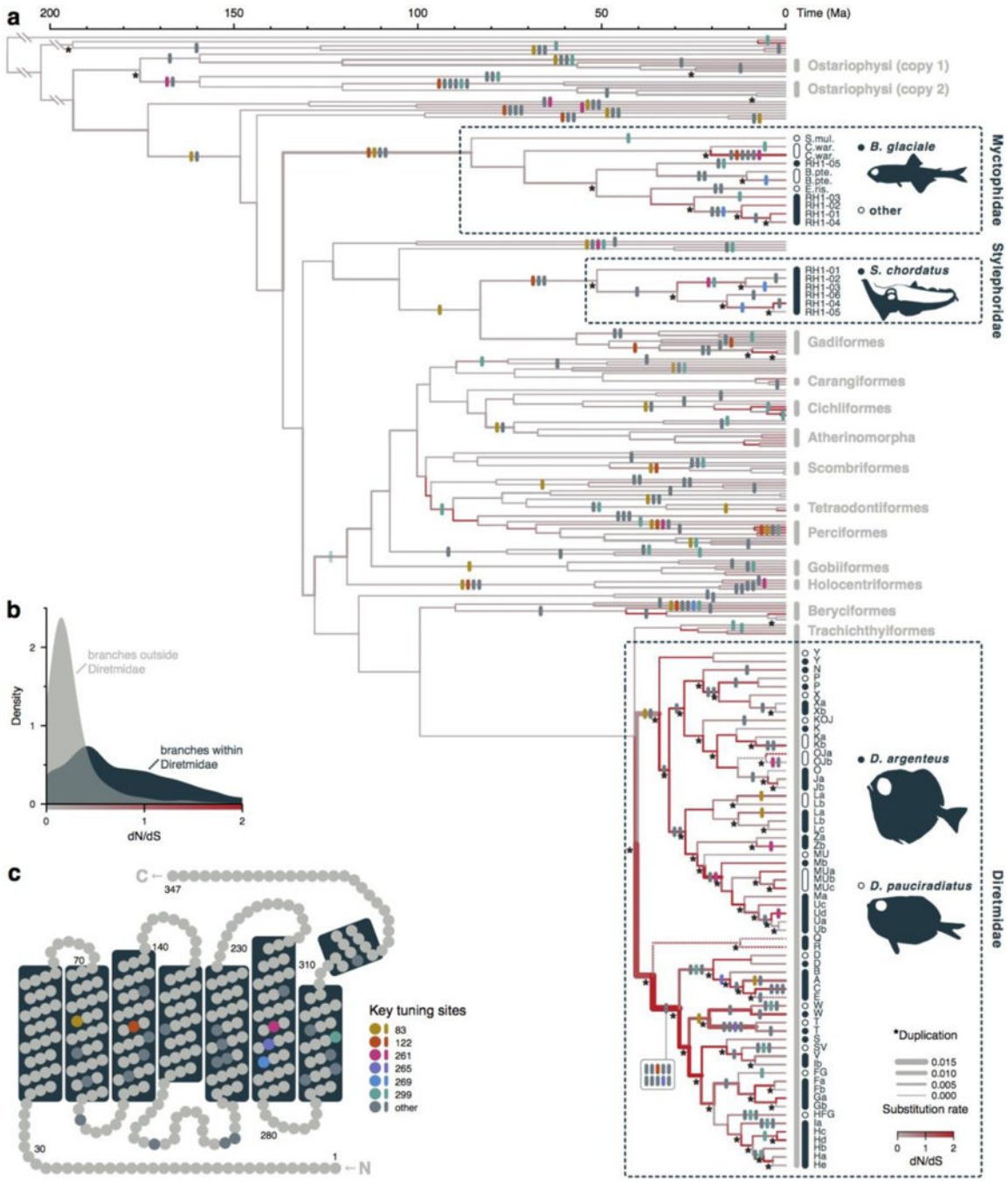

Fig. 3. Evolution and functional diversification of RH1 in deep-sea fishes.

(**A**) Time-calibrated gene tree based on teleost *RH1s* demonstrating lineage-specific duplications in three deep-sea fish lineages. Vertical bars indicate amino acid substitutions in key spectral-tuning sites (1,3). Gene duplication events are marked with an asterisk. The branches in the gene tree are color-coded according to the rate of non-synonymous to synonymous substitutions (dN/dS); each branch's thickness refers to the reconstructed substitution rate. (**B**) Distribution of the per-branch dN/dS-values within the *RH1s* of Diretmidae compared to all other branches in the teleost *RH1* gene tree based on ancestral

sequence reconstructions. (**C**) Basic model of the RH1 protein showing its seven trans-membrane helices and the positions of known key spectral-tuning sites including the disulfide bridge reported here.